MODELING WOOD MOISTURE SORPTION HYSTERESIS BASED ON SIMILARITY HYPOTHESIS. PART 1. DIRECT APPROACH

Perry N. Peralta
Assistant Professor

and

Audimar P. Bangi
Researcher

Department of Wood and Paper Science
North Carolina State University
Raleigh, NC 27695-8005

(Received June 1997)

ABSTRACT

A similarity-hypothesis approach to modeling sorption hysteresis in porous media has been applied to wood. The method, which uses the adsorption and desorption relative humidities directly as similarity statement parameters, is simpler than previously reported techniques based on the independent-domains theory since only the boundary curves of the main hysteresis loop are required in order to generate the scanning curves at a given temperature. A comparison of the predicted scanning curves with actual experimental data for yellow-poplar (*Liriodendron tulipifera*) indicates that the approach is highly reliable, with predicted values within 0.01 to 1.05 of the actual equilibrium moisture content of the samples at different relative humidity levels.

Keywords: Modeling, independent-domains theory, similarity hypothesis, sorption, adsorption, desorption, isotherm, hysteresis, yellow-poplar, *Liriodendron tulipifera.*

INTRODUCTION

Existing data on the sorption behavior of wood provide desorption and adsorption curves from the green and fully dry initial conditions, respectively. Wood in actual use, however, is exposed only to a very narrow range of relative humidities and, therefore, should exhibit isotherms different from the full cycle isotherms. To illustrate this point, consider a yellow-poplar sample initially at the oven-dry condition when placed in a conditioning chamber set at 30°C. If the sample is subjected to increasing relative humidities, it will be gaining moisture, with its equilibrium moisture content (EMC) at each relative humidity (H) increment being given by the dashed curve in Fig. 1 (Peralta 1995a). At 55% H, for instance, the piece of wood will have an EMC of about 8.3%. If at this point the relative humidity is decreased to 50% and then further to 45%, the material will be in a desorption process. To obtain the moisture content of the wood at this point, it is tempting to use the desorption curve in Fig. 1, which at 45% H gives an EMC of 8.6%. This is obviously a wrong approach, since the sample should now have a moisture content lower than 8.3%, its EMC just before desorption.

The above phenomenon can be attributed to the fact that the desorption and adsorption isotherms over the full range of relative humidity (called boundary isotherms) simply define the delimiting loop that encloses the hysteresis region (Urquhart 1960). If the direction of sorption is reversed at any point along a boundary isotherm, an intermediate curve (called scanning isotherm) will be traced (Peralta 1995a). Just like the boundary curves, the scanning isotherms also exhibit hysteresis. Since experimental sorption data are often very limited and time-consuming to generate, a reliable

Wood and Fiber Science, 30(1), 1998, pp. 48–55

means of predicting hysteresis trends commencing at any reversal point along the sorption boundary loop would be a valuable tool for anyone involved in practical wood-moisture relations.

In two previous papers (Peralta 1995b, 1996), the feasibility of mathematically modeling wood moisture sorption hysteresis based on the Neel-Everett theory of independent domains was explored using the sorption data for yellow-poplar (*Liriodendron tulipifera*). The method, similar to that employed by Poulovassilis (1962), requires experimental boundary isotherms and a family of primary scanning curves to predict the EMC-H relationship. Mualem (1973, 1974) presented two models based on similarity hypothesis that require only the boundary isotherms at a given temperature in order to predict any scanning curve of interest at that temperature. This paper (Part 1) looks at the applicability to wood of Mualem's first model, which uses the adsorption and desorption relative humidities (H_{12} and H_{21}) directly as parameters in the similarity statement. An accompanying paper (Part 2) evaluates the second model, which employs the capillary system's geometry to reflect both the reversible and irreversible components of the sorption process. The papers were written to parallel each other so that readers could easily compare the two models. If found suitable, the models could provide simple tools for predicting EMC-H relations for wood.

THEORETICAL CONSIDERATION

Based on the concept of independent domains, the amount of water M present in a piece of wood is given by the equation (Peralta 1995b, 1996):

$$M = \iint w(H_{12}, H_{21})\, dH_{21}\, dH_{12} \qquad (1)$$

where H_{12} and H_{21} are independent variables representing the relative humidities for adsorption and desorption, respectively; and $w(H_{12}, H_{21})\, dH_{21}\, dH_{12}$ represents the amount of water

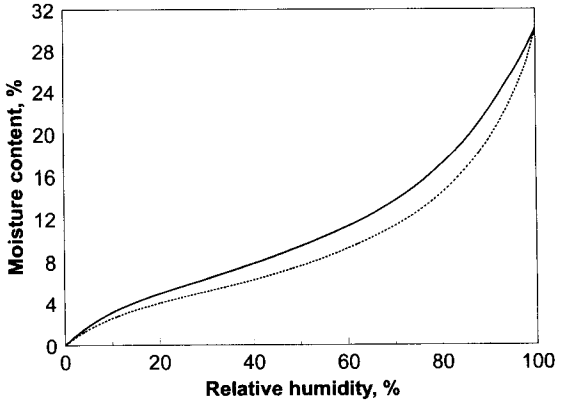

FIG. 1. Adsorption (– – –) and desorption (———) isotherms for yellow-poplar at 30°C.

in domains having transition points in the rectangle $dH_{12}\, dH_{21}$ near (H_{12}, H_{21}). According to Mualem (1973), the moisture distribution function $w(H_{12}, H_{21})$ is a bivariate distribution that may be represented as the product of two independent distribution functions $h(H_{12})$ and $l(H_{21})$ so that

$$w(H_{12}, H_{21}) = h(H_{12})\, l(H_{21}). \qquad (2)$$

Equation (2) embodies the mathematical expression of Mualem's version of the similarity hypothesis, which resembles that of Philip's (1964) but is much simpler to implement mathematically. The physical meaning of the above equation can be visualized by examining Figs. 2b and 2d. As reflected in the plane (H_{12}, H_{21}) of Figs. 2b and 2d, the contributions of domains lying on the vertical line AB are distributed in proportion to the distribution function $l(H_{21})$, while the contributions of domains lying along the horizontal line DE are distributed in proportion to the function $h(H_{12})$. According to the similarity hypothesis, the distribution along a given vertical line is identical to that along other vertical lines except for the constant factor $h(H_{12})$. In the same manner, the distributions along different horizontal lines are identical, except for the constant factor $l(H_{21})$.

Mualem (1973) then defined two integral functions $\eta(H)$ and $\lambda(H)$ based on $h(H_{12})$ and $l(H_{21})$, respectively, as follows:

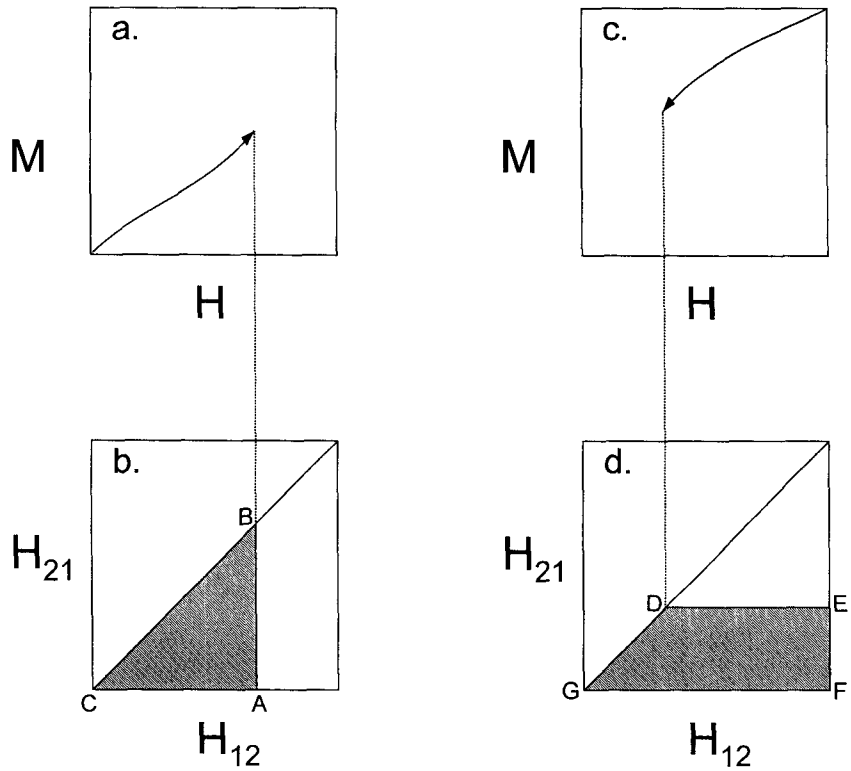

FIG. 2. Adsorption (a) and desorption (c) boundary isotherms with their corresponding states of domains (b and d, respectively).

$$\eta(H) = \int_0^H h(H)\, dH \tag{3}$$

$$\lambda(H) = \int_0^H l(H)\, dH. \tag{4}$$

It is apparent from Eq. (3) that

$$\eta(0) = \int_0^0 h(H)\, dH = 0 \tag{5a}$$

and

$$\eta(100) = \int_0^{100} h(H)\, dH = \text{constant}. \tag{5b}$$

Since $\eta(100)$ is constant, its value may be chosen arbitrarily. To normalize the function $h(H)$, Mualem (1973) took $\eta(100) = 1$.

The functional relationship between the moisture content for the adsorption boundary curve M_a and relative humidity H (Fig. 2a) is obtained by integrating the moisture distribution function over the filled domains depicted by the triangle ABC in Fig. 2b:

$$M_a(H) = \int_0^H h(H_{12}) \left[\int_0^{H_{12}} l(H_{21})\, dH_{21} \right] dH_{12}. \tag{6}$$

Incorporating the integral function $\lambda(H)$ results in

$$M_a(H) = \int_0^H h(H_{12}) \lambda(H_{12})\, dH_{12} \tag{7}$$

and

$$dM_a(H) = h(H)\, \lambda(H)\, dH. \tag{8}$$

The same approach can be used to obtain the relationship between the moisture content

for the desorption boundary curve M_d and relative humidity H (Fig. 2c), that is, by integrating over the filled domains depicted by the trapezoid DEFG in Fig. 2d:

$$M_d(H) = \\ = M_a(H) + \int_H^{100} h(H_{12})\, dH_{12} \int_0^H l(H_{21})\, dH_{21}. \quad (9)$$

Substituting the integral functions $\eta(H)$ and $\lambda(H)$ from Eqs. (3) and (4) in Eq. (9), gives

$$M_d(H) = M_a(H) + [1 - \eta(H)]\lambda(H) \quad (10)$$

and

$$dM_d(H) = [1 - \eta(H)]l(H)\, dH. \quad (11)$$

Equation (10) can be written as

$$\lambda(H) = \frac{M_d(H) - M_a(H)}{1 - \eta(H)} \quad (12)$$

so that substituting the above expression in Eq. (8) results in the relation

$$\frac{dM_a(H)}{M_d(H) - M_a(H)} = \frac{h(H)\, dH}{1 - \eta(H)}. \quad (13)$$

Integration of Eq. (13) leads to

$$\int_0^H \frac{dM_a(H)}{M_d(H) - M_a(H)} = -\ln[1 - \eta(H)] \quad (14)$$

or

$$\eta(H) = 1 - \exp\left(-\int_0^H \frac{dM_a(H)}{M_d(H) - M_a(H)}\right). \quad (15)$$

By defining the function

$$F(H) = \int_0^H \frac{dM_a(H)}{M_d(H) - M_a(H)}, \quad (16)$$

Eq. (15) can be simplified to the form

$$\eta(H) = 1 - \exp[-F(H)] \quad (17)$$

and, once the above equation is solved, the function $\lambda(H)$ can be determined by using Eq. (12).

METHODOLOGY AND RESULTS

The suitability of Mualem's model based on direct-similarity hypothesis to wood sorption hysteresis was tested by comparing the predicted moisture content values with actual experimental data for yellow-poplar. The equations for different scanning curves were expressed in terms of the functions $\eta(H)$ and $\lambda(H)$. Using a notation suggested by Enderby (1955), the primary desorption scanning curves were generated using the relation

$$M\begin{pmatrix} H_{121} \\ 0 \quad H_{21x} \end{pmatrix} = \\ = M_a(H_{12x}) + \int_0^{H_{21x}} \int_{H_{12x}}^{H_{121}} w\, dH_{12}\, dH_{21}$$

which simplifies to the form

$$M\begin{pmatrix} H_{121} \\ 0 \quad H_{21x} \end{pmatrix} = \\ = M_a(H_{12x}) + \lambda(H_{21x})[\eta(H_{121}) - \eta(H_{12x})], \quad (18)$$

where M is the moisture content of interest; the notation in parentheses on the left side of the equation describes the dynamics of the sorption process, that is, H first increases from 0 to H_{121} and then decreases from H_{121} to $H_{21}x$ (Figs. 3a and 3b); H_{121} the relative humidity corresponding to the reversal point of the given primary desorption scanning isotherm; H_{12x} ($=H_{21x}$) the relative humidity corresponding to M during adsorption; H_{21x} ($=H_{12x}$) the relative humidity corresponding to M during desorption; and $M_a(H_{12x})$ the moisture content on the adsorption boundary curve corresponding to H_{12x}. The results of the computations using Eq. (18) were compared with actual experimental sorption data for yellow-poplar and are presented in Table 1.

Using the same relations, the primary adsorption scanning curves (although not determined experimentally in this study) can be established using the equation

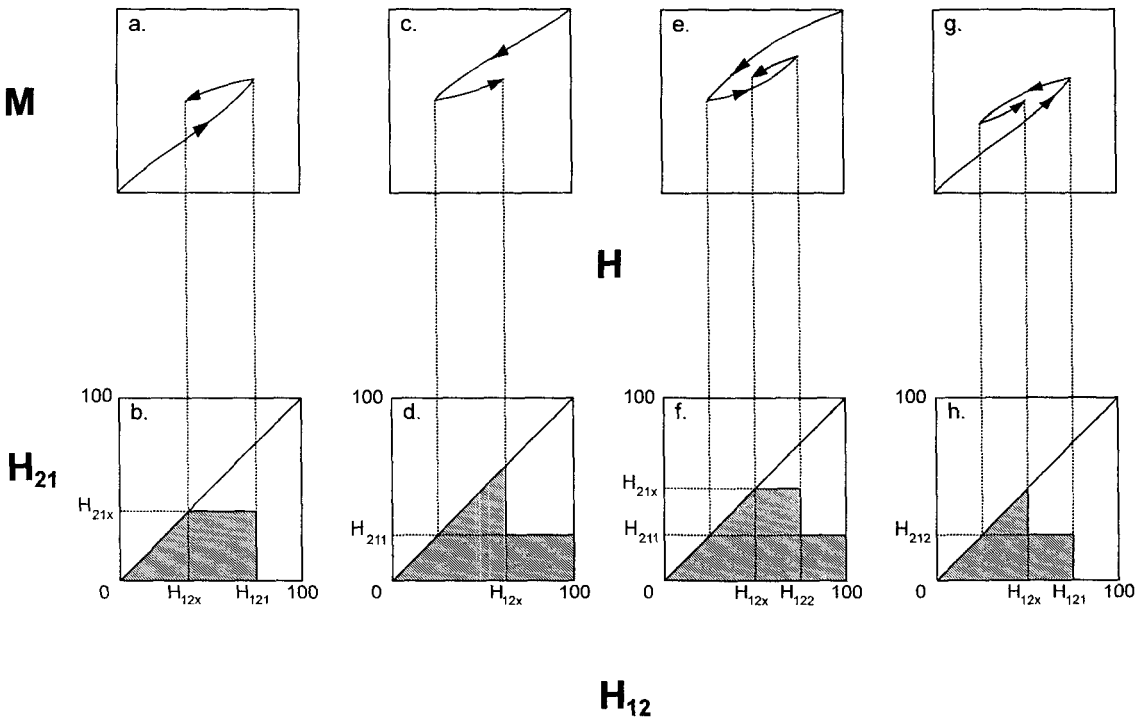

FIG. 3. Primary desorption (a), primary adsorption (c), secondary desorption (e), and secondary adsorption (g) scanning isotherms with their corresponding states of domains (b, d, f, and h, respectively).

$$M\begin{pmatrix} 100 & H_{12x} \\ & H_{211} \end{pmatrix} = \\ = M_a(H_{12x}) + \lambda(H_{211})[1 - \eta(H_{12x})] \quad (19)$$

where the notation in parentheses following M indicates that H decreases from *100* to H_{211} and then increases from H_{211} to H_{12x} (Figs. 3c and 3d); H_{211} is the relative humidity corresponding to the reversal point of the given primary adsorption scanning isotherm; and the rest of the terms are as previously defined. The secondary desorption (Figs. 3e and 3f) and secondary adsorption (Figs. 3g and 3h) scanning curves can likewise be established using the following relations, respectively:

$$M\begin{pmatrix} 100 & H_{122} \\ H_{211} & H_{21x} \end{pmatrix} = \\ = M_a(H_{12x}) + \lambda(H_{21x})[\eta(H_{122}) - \eta(H_{12x})] + \\ + \lambda(H_{211})[1 - \eta(H_{122})] \quad (20)$$

$$M\begin{pmatrix} H_{121} & H_{12x} \\ 0 & H_{212} \end{pmatrix} = \\ = M_a(H_{12x}) + \lambda(H_{212})[\eta(H_{121}) - \eta(H_{12x})] \quad (21)$$

where H_{122} and H_{212} are the relative humidity corresponding to the reversal point of the secondary desorption and secondary adsorption scanning isotherms, respectively; and the rest of the terms are as previously defined.

In all the above cases, the relationship between moisture content and relative humidity is expressed in terms of $M_a(H)$, $\eta(H)$, and $\lambda(H)$. The values of $M_a(H)$, $\eta(H)$, and $\lambda(H)$ for yellow-poplar, together with intermediate parameters $M_d(H)$ and $F(H)$, were calculated at 2% relative humidity intervals from 0 to 100%. The desorption and adsorption boundary isotherms were calculated using the Hailwood-Horrobin equation whose parameters (M_p, K_1, and K_2) are listed in Table 2 of Peralta

TABLE 1. *Comparison of model-based and experimentally determined moisture contents of yellow-poplar for the different primary desorption scanning isotherms.*

Relative humidity (%)	Moisture content (%)											
	Scanning 92[a]			Scanning 75[a]			Scanning 53[a]			Scanning 32[a]		
	Model	Expt.	Error	Model	Expt.	Error	Model	Expt.	Error	Model	Expt.	Error
11	3.34	3.16	0.18	3.34	3.11	0.23	3.33	3.06	0.27	3.31	2.98	0.33
22	5.24	5.14	0.10	5.23	5.00	0.23	5.17	4.83	0.34	4.87	4.62	0.25
32	6.67	6.62	0.05	6.64	6.50	0.14	6.43	6.17	0.26			
43	8.25	8.41	−0.16	8.17	8.19	−0.02	7.53	7.54	−0.01			
53	9.88	10.11	−0.23	9.67	9.73	−0.06						
63	11.87	11.84	0.03	11.28	11.00	0.28						
75	15.06	14.46	0.60									
84	18.30	17.25	1.05									

[a] Scanning 92, Scanning 75, Scanning 53, and Scanning 32 refer to the primary desorption scanning curve whose reversal point corresponds to relative humidity of 92, 75, 53, and 32%, respectively.

(1995a). (Note: M_p for the adsorption boundary isotherm should be 352.677 instead of 362.677.) These isotherms were extended to 100% relative humidity by extrapolating the equations and taking the average (30.13% moisture content) of the extrapolated values as the upper closure point of the hysteresis loop. The integral function $F(H)$ was calculated using the trapezoidal rule of numerical integration.

DISCUSSION AND CONCLUSIONS

From Eqs. (12) and (16), it becomes apparent that problematic points lie at the two ends of the main hysteresis loop, where singularities occur. As M_a approaches 0 (or H approaches 0), the graph of $1/(M_d - M_a)$ vs. M_a tends towards infinity such that F is infinite at all values of M_a. But for Mualem's approach to be valid, F must be finite so that the functions $\eta(H)$ and $\lambda(H)$ will also be finite. To resolve this conflict, a finite value of $1/(M_d - M_a)$ at $M_a = 0$ was obtained by performing a second-order polynomial regression on the $(1/(M_d - M_a))$ vs. M_a data for $H = 2$, 4, 6, and 8%. The y-intercept (=14.82) was then used as the value of $1/(M_d - M_a)$ at $M_a = 0$. At the other end of the relative humidity range, a similar problem was encountered. As H approaches 100%, F should approach infinity so that the condition $\eta(100) = 1$ will be met. As it turned out in the calculations of the scanning curves for yellow-poplar, this requirement is not particularly restrictive since even at low relative humidities (H as low as 5%), $F > 10$ such that $\eta = 1 - e^{-10} = 0.999955$. For the yellow-poplar data, F increased monotonically from 0 at 0% relative humidity to 27.88 at 98% relative humidity. Fitting a quadratic equation to the last five data points (H = 90, 92, 94, 96, 98) yielded an R^2 of 0.996. Extrapolation of the curve to 100% relative humidity resulted in an F value of 29.41. Thus, $\eta = 1 - e^{-29.41} \approx 1$.

Mualem's model based on direct-similarity hypothesis must be evaluated in terms of its compatibility with the requirement of the independent-domain theory that the moisture distribution function $w(H_{12}, H_{21})$ be always positive. This implies then that the functions $h(H)$ and $l(H)$ be both positive or both negative. Combining Eqs. (3) and (17) results in

$$h(H) = \frac{d\eta(H)}{dH} = e^{-F(H)}\frac{dF(H)}{dH}. \quad (22)$$

Since $F(H)$ is monotonically increasing (Fig. 4) and since the range of the natural exponential function is a set of nonnegative real numbers, then $h(H)$ is positive in the range $0 \leq H \leq 100$. Positive values of h over the full range of relative humidity require that the graph relating η with H be monotonically increasing. This was confirmed in the study wherein η

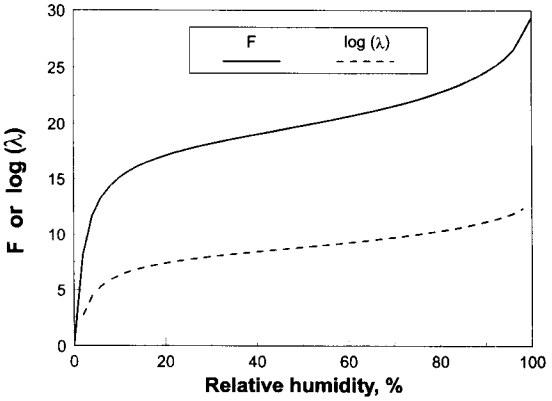

FIG. 4. The integral function F and the logarithm of the integral function λ for yellow-poplar at different relative humidity levels. The integral function $\eta = 1 - \exp(-F)$.

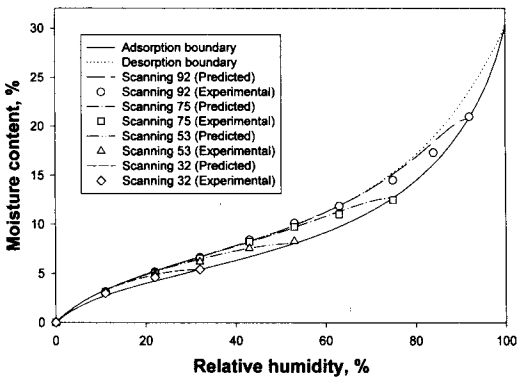

FIG. 5. Primary desorption scanning isotherms predicted by the model based on direct-similarity hypothesis (dashed curves) and the experimentally-determined data points (symbols) for yellow-poplar. Scanning 92, Scanning 75, Scanning 53, and Scanning 32 refer to the primary desorption scanning curve whose reversal point corresponds to relative humidity of 92, 75, 53, and 32%, respectively.

was found to increase from 0 to 1 as H increased from 0 to 100%.

Also, from Eq. (11), it follows that

$$l(H) = [1 - \eta(H)]^{-1} \frac{dM_d(H)}{dH}. \qquad (23)$$

Since $0 \leq \eta \leq 1$ and $dM_d(H)/dH \geq 0$, then it is clear that l is also positive in the range $0 \leq H \leq 100$. Figure 4 reveals that the graph relating λ with H is monotonically increasing, again confirming that its derivative l is positive over the full range of relative humidity. Hence, it appears that the model, as applied to wood moisture sorption, is compatible with the general theory of independent domains.

Table 1 shows that predictions based on the model are relatively close to the experimental data points for yellow-poplar, with percent moisture content prediction errors ranging from 0.01 to 1.05. The goodness of fit of the predicted desorption scanning curves relative to the experimentally generated points is exhibited in Fig. 5. Since the weights of the samples were measured to the nearest 0.05 mg and the oven-dry weights of the samples were approximately 0.560 g, the discrepancies noted are certainly greater than the moisture content determination error of 0.01% MC. Some of the observed discrepancies may have resulted from other measurement errors like those for relative humidity determinations.

Figure 5 shows that the slopes of the predicted primary desorption scanning curves immediately after each reversal are equal to zero. This is a consequence of the fact that the contribution of capillaries that behave reversibly during sorption is not incorporated in the model. Although the independent-domain theory recognizes the existence of such capillaries, Mualem's direct-similarity formulation of the theory does not include a term describing the behavior of those capillaries. The experimental primary desorption scanning curve with reversal point of 92% H exhibits the characteristic sigmoid shape of sorption isotherms (Peralta 1995a) and therefore does not have a zero slope immediately after sorption reversal. The other experimental scanning isotherms when fitted with quadratic type equations (Peralta 1995a) also reveal non-zero slopes at reversal.

In conclusion, Mualem's model based on direct-similarity hypothesis is compatible with the theory of independent domains. Although only the irreversible component of sorption is accounted for by the model, the predicted curves showed good agreement with experimentally measured data, indicating that Mu-

alem's method is adequate and simple enough to be considered as a practical tool for wood moisture sorption analysis. Overall, the model possesses the following useful properties: (1) it requires only the two boundary isotherms to predict any desired scanning curve for a particular wood species at a given temperature; and (2) it enables the scanning curves to be defined in analytical form and to consistently fall within the boundary hysteresis loop.

REFERENCES

ENDERBY, J. A. 1955. The domain model of hysteresis. Part 1. Independent domains. Trans. Faraday Soc. 51: 835–848.

MUALEM, Y. 1973. Modified approach to capillary hysteresis based on a similarity hypothesis. Water Resources Res. 9(5):1324–1331.

———. 1974. A conceptual model of hysteresis. Water Resources Res. 10(3):514–520.

PERALTA, P. N. 1995a. Sorption of moisture by wood within a limited range of relative humidities. Wood Fiber Sci. 27(1):13–21.

———. 1995b. Modeling wood moisture sorption hysteresis using the independent-domain theory. Wood Fiber Sci. 27(3):250–257.

———. 1996. Moisture sorption hysteresis and the independent-domain theory: The moisture distribution function. Wood Fiber Sci. 28(4):406–410.

PHILIP, J. R. 1964. Similarity hypothesis for capillary hysteresis in porous materials. J. Geophys. Res. 69(8): 1553–1562.

POULOVASSILIS, A. 1962. Hysteresis of pore water: An application of the concept of independent domains. Soil Sci. 93:405–412.

URQUHART, A. R. 1960. Sorption isotherms. Pages 14–32 *in* J. W. S. Hearle and R. H. Peters, eds. Moisture in textiles. Wiley Interscience, New York, NY.